

Measurement of Magnetization Dynamics in Single-Molecule Magnets Induced by Pulsed Millimeter-Wave Radiation

M. Bal and Jonathan R. Friedman

Department of Physics, Amherst College, Amherst, Massachusetts 01002-5000, USA

M. T. Tuominen

Department of Physics, University of Massachusetts, Amherst, Massachusetts 01003, USA

E. M. Rumberger and D. N. Hendrickson

Department of Chemistry and Biochemistry, University of California at San Diego, La Jolla, California 92093, USA

(Dated: April 14, 2024)

We describe an experiment aimed at measuring the spin dynamics of the Fe_8 single-molecule magnet in the presence of pulsed microwave radiation. In earlier work, heating was observed after a 0.2-ms pulse of intense radiation, indicating that the spin system and the lattice were out of thermal equilibrium at millisecond time scale [Bal et al., *Europhys. Lett.* **71**, 110 (2005)]. In the current work, an inductive pick-up loop is used to probe the photon-induced magnetization dynamics between only two levels of the spin system at much shorter time scales (from ns to μs). The relaxation time for the magnetization, induced by a pulse of radiation, is found to be on the order of 10 μs .

Single-molecule magnets are unique systems that lie at the border between the classical and quantum worlds. Like classical magnets, they are bistable and exhibit hysteresis at low temperatures.^{1,2} They also exhibit fascinating quantum mechanical properties, such as tunneling between “up” and “down” orientations,^{3,4,5} and interference between tunneling paths.⁶ Furthermore, their potential use in quantum computation has been proposed,⁷ and experiments with millimeter-wave radiation have demonstrated an enhancement in the relaxation rate for magnetization reversal,^{8,9} as well as induced changes in the equilibrium magnetization.^{10,11,12,13,14}

Recent work has focused on measuring the spin relaxation time T_1 and the decoherence time T_2 .^{10,12,15,16} Determination of these parameters as well as exploration of coherent spin dynamics are important in order to see if single-molecule magnets can be employed as qubits.⁷ In previous work, the speed of the micro-Hall-bar detectors used prevented the measurement of magnetization relaxation at time scales shorter than a few microseconds.¹⁰ In this paper, we use a thin-film inductive pick-up loop as a fast flux detector. This method, however, has the drawback of reduced sensitivity when compared to the Hall sensor.

We study the single-molecule magnet $\text{Fe}_8\text{O}_2(\text{OH})_{12}(\text{tacn})_6$ (hereafter called Fe_8), which is composed of eight magnetic Fe(III) ions strongly coupled together to form a single spin-10 system and is described by the effective Hamiltonian

$$H = D S_z^2 + E (S_x^2 - S_y^2) + C (S_+^4 + S_-^4) - g_B S_z H; \quad (1)$$

where the anisotropy constants D , E , and C are 0.292 K, 0.046 K, and 2.9×10^{-5} K, respectively, and $g = 2$.^{6,17,18,19} The first (and largest) term causes the spin to prefer to lie along or opposite the z axis, resulting in a double-well potential, and making the energy levels approximately the eigenstates of S_z . The second and third terms break the rotational symmetry of the Hamiltonian and result in tunneling between the otherwise unperturbed states. Reversal of the magnetization from one easy-axis direction to another is impeded by a 25 K barrier.⁵

As a radiation source we use either a solid-state multiplier fed by a frequency synthesizer or a high-power backward-

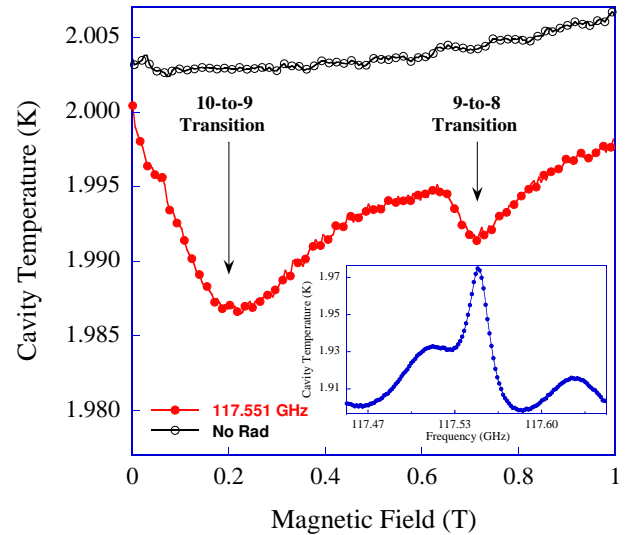


FIG. 1: (Color online) Cavity temperature as a function of magnetic field, both in the presence and absence of continuous-wave radiation. Transitions are observed from the $m = 10$ level to the $m = 9$ level, as well as from $m = 9$ to $m = 8$, as indicated. The resonant frequency of the cavity is determined by monitoring the cavity temperature, as shown in the inset. When on resonance the temperature rises sharply because radiation enters the cavity. The variation of the cavity temperature away from the resonance is due to the variation of the output power of the microwave source with frequency.

wave oscillator (BWO). The radiation propagates in a rectangular stainless-steel WR-10 waveguide with gold plating on the inner surfaces. Our resonator is a cylindrical cavity made of oxygen-free copper with dimensions of 3.17 mm \times 4.62 mm (diameter \times length). Some resonances, such as the $\text{TE}_{0,1,1}$ mode, of a cylindrical cavity do not require an ac current to flow between the end plates and the walls, resulting in very high quality factors (on the order of 10^4 in the present study).²⁰ Finally, a thin-film pick-up loop on a silicon substrate serves as our detector for measuring changes in magnetic field originating from a single crystal of Fe_8 placed inside the cavity. The pick-up loop is fabricated using standard electron-beam lithography, followed by metal deposition (thermally evaporated Cu film) and lift-off. A rectangular loop

(65 205 m²) is defined by 5- m-wide and 200-nm-thick Cu lines.

Radiation is coupled to the cavity through a small hole in the top plate of the cavity. A 25- m-thick gold foil forms the bottom plate. A 0.5-mm-diameter hole is made in the Au foil and the pickup loop is placed just beneath this hole. The hole allows the fast magnetization signal from the sample to couple to the loop without attenuation and also permits the sample to be positioned as close as possible to the pick-up loop. In some experiments, a thin piece of Mylar foil coated with 50 nm of amorphous copper is placed between the sample and loop. The copper film is much thicker than the skin depth of the radiation, allowing the foil to form a good electromagnetic closure for the cavity at microwave frequencies. At the same time, the film is thinner than the skin depth at the time scales of the sample magnetization signals, allowing them to couple through the film without significant attenuation. The external magnetic field is applied along the axis of the cylindrical cavity and perpendicular to the microwave field at the sample location.

The Fe₈ sample is mounted such that its crystallographic b-axis is parallel to the substrate surface of the pick-up loop. The loop dimensions were chosen to match the typical size of a single crystal. Both of these considerations allow for maximum flux coupling. However, the sample mounting technique results in a large angle (typically around 35 to 45 °) between the easy-axis of the magnetization and the applied magnetic field. The induced emf in our pick-up loop is directly proportional to the rate of change in the magnetization (dM/dt) of the Fe₈ sample. We also did experiments with the sample's a-axis parallel to the external field (in order to reduce the angle between the easy axis and the field to 15 °), but were unable to measure a signal because the flux coupling was too weak.

We determined the resonant frequency of the cavity by monitoring the cavity temperature while sweeping the frequency of the radiation. The finite conductivity of the cavity walls results in ohmic heating when on resonance and is registered by our thermometer (mounted outside the cavity), as shown in the inset of Figure 1. This resonance, at 117.551 GHz, corresponds to the TE_{0,1,1} mode of the cylindrical cavity and has a quality factor of 9800.

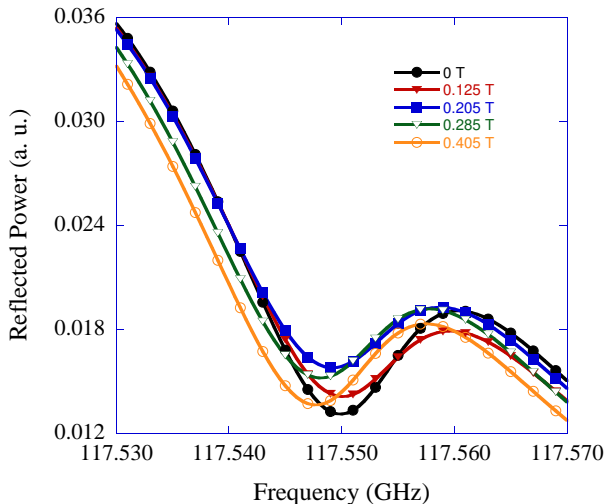


FIG. 2: (Color online) Reflected power from the cavity is measured as a function frequency and is plotted for several constant magnetic field as indicated on the plot.

The pick-up loop is not a suitable detector of slowly varying magnetic signals and therefore is not useful to perform spectroscopic studies. Measuring the cavity temperature, on the other hand, as a function of the magnetic field allowed us to perform crude spectroscopic measurements. In Figure 1, the cavity temperature is shown as a function of magnetic field and clearly changes when the resonance condition for the Fe₈ sample is satisfied (10-to-9 and 9-to-8 transitions are shown); the measurement taken in the absence of radiation is shown for comparison. It should be noted, however, that the cavity temperature in Fig.1 decreases when the sample is on resonance with the radiation, in contrast to the heating observed in our previous experiment.¹⁰ This unexpected behavior required us to study the properties of the cavity in greater detail. Figure 2 shows the microwave power reflected from the cavity, using a directional coupler and diode detector, as a function of frequency at several constant magnetic fields. The microwave power reflected from the cavity changes as we field tune the Fe₈ sample through the 10-to-9 transition. In other words, the power absorption by the cavity is minimized when the resonance condition is met. A frequency shift of a few MHz is also present but does not seem to depend on whether the sample is on resonance with the radiation. The decrease in cavity temperature can be explained as a consequence of a decrease in the absorbed microwave power by the cavity, which in turn is caused by the sample coming to resonance with the cavity. These observations suggest that tuning the sample to resonance with the cavity adds a dispersive element to the cavity and thereby changes the impedance matching condition between the waveguide and the cavity. Similar cavity-sample interactions form the basis of electron-spin-resonance spectrometers in which a resonant cavity can be operated either in the absorption mode (quality factor change) or in the dispersion mode (frequency change).²¹

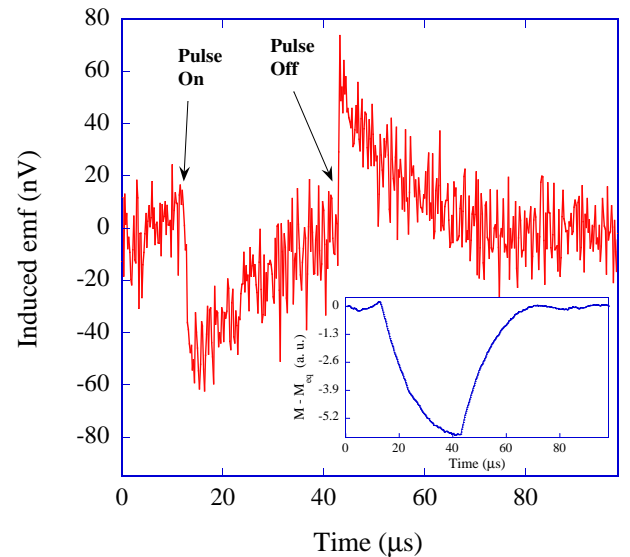


FIG. 3: (Color online) The induced emf (proportional to dM/dt) in the pick-up loop is plotted as a function of time. The inset shows the magnetization, calculated by numerically integrating the induced emf, as a function of time.

A PIN-diode switch is employed to pulse the microwave radiation. The radiation frequency is set to the cavity resonance as described above. The field is set 0.19 T so that the transition from the ground to the first excited state of the Fe₈ sample

is resonant with the radiation (Fig. 1). A 30- μ s radiation pulse is applied and repeated every 10 ms at a temperature of 1.8 K. A fast digitizing oscilloscope is used to capture the induced emf from the pick-up loop after passing through a fast, low-noise preamp. Figure 3 shows the induced emf as a function of time; the data contains the average of 3.84×10^5 individual traces to increase the signal-to-noise ratio. The inset shows the sample magnetization as a function of time, obtained by numerically integrating the data in the main part of the figure. The induced emf (and thereby dM/dt) exhibits sharp jumps when the radiation is turned on and off. The sharp jumps indicate that the radiation immediately causes the magnetization to start decreasing and that it begins to increase as soon as the radiation is turned off, as shown in the inset. The rate of magnetization change decays to zero in a time of roughly 10 μ s. After such a time, the magnetization has achieved a nearly steady state.

We tentatively interpret these results in terms of the spin dynamics of the two levels involved in the radiative transition. Turning on the radiation initiates photon-induced transitions from $m = 10$ to 9,²² resulting in a decrease in the magnetization. After a steady state is reached, the $m = 9$ state has a larger population than under thermal equilibrium conditions and the excess population decays back to the ground state once the radiation is turned off. The 10- μ s relaxation time is

surprisingly long for spin-phonon interactions, which presumably determine the time scale of the observed decays. Further study of the spin dynamics in the presence of pulsed radiation is needed to understand the origin of this long relaxation time.

In conclusion, we have built a cryogenic millimeter-wave probe to measure the fast magnetization dynamics of single-molecule magnets in the presence of pulsed, resonant radiation. A cylindrical cavity with a high quality factor and a thin-film inductive pick-up loop are used to study the time evolution of the magnetization of Fe_8 during and after a single pulse of millimeter-wave radiation. We find an unusually long relaxation time of 10- μ s. A poor signal-to-noise ratio requires the averaging of a large number of traces, which currently demands extremely long experimental run times. Modifications to the experimental set-up to improve the signal-to-noise ratio are in progress.

We thank M. P. Sarachik, Y. Suzuki, D. DeMille, J. Tu, D. Hall, L. Hunter, and K. Mertes for useful conversations. We also thank D. Krause and G. Gallo for their technical contributions to this study. We are also grateful to M. Foss-Feig, E. da Silva Neto, and J. Rasowsky for their help in acquiring and analyzing some of the data. Support for this work was provided by the US National Science Foundation, the Research Corporation, the Alfred P. Sloan Foundation, and the Center of Excellence of the Israel Science Foundation.

* Corresponding author. E-mail: jrfriedman@amherst.edu

- ¹ R. Sessoli, D. Gatteschi, A. Caneschi, and M. A. Novak, *Nature* **365**, 141-143 (1993).
- ² D. Gatteschi, A. Caneschi, L. Pardi, and R. Sessoli, *Science* **265**, 1054-1058 (1994).
- ³ J. R. Friedman, M. P. Sarachik, J. Tejada, and R. Ziolo, *Phys. Rev. Lett.* **76**, 3830-3833 (1996).
- ⁴ L. Thomas, F. Lioni, R. Ballou, D. Gatteschi, R. Sessoli, and B. Barbara, *Nature* **383**, 145-147 (1996).
- ⁵ C. Sangregorio, T. Ohm, C. Paulsen, R. Sessoli, and D. Gatteschi, *Phys. Rev. Lett.* **78**, 4645-4648 (1997).
- ⁶ W. Wernsdorfer and R. Sessoli, *Science* **284**, 133-135 (1999).
- ⁷ M. N. Leuenberger and D. Loss, *Nature* **410**, 789-793 (2001).
- ⁸ R. Amigó, J. M. Hernandez, A. García-Santiago, and J. Tejada, *Phys. Rev. B* **67**, 220402(R) (2003).
- ⁹ L. Sorace, W. Wernsdorfer, C. Thirion, A.-L. Barra, M. Pacchioni, D. Mailly, and B. Barbara, *Phys. Rev. B* **68**, 220407 (2003).
- ¹⁰ M. Bal, J. R. Friedman, Y. Suzuki, E. M. Rumberger, D. N. Hendrickson, N. Avraham, Y. Myasoedov, H. Shtrikman, and E. Zeldov, *Europhys. Lett.* **71**, 110-116 (2005).
- ¹¹ W. Wernsdorfer, A. Mueller, D. Mailly, and B. Barbara, *Europhys. Lett.* **66**, 861-867 (2004).
- ¹² E. del Barco, A. D. Kent, E. C. Yang, and D. N. Hendrickson, *Phys. Rev. Lett.* **93**, 157202 (2004).
- ¹³ M. Bal, J. R. Friedman, Y. Suzuki, K. M. Mertes, E. M. Rumberger, D. N. Hendrickson, Y. Myasoedov, H. Shtrikman, N. Avraham, and E. Zeldov, *Phys. Rev. B* **70**, 100408(R) (2004).

- ¹⁴ B. Cage, S. E. Russek, D. Zipse, J. M. North, and N. S. Dalal, *Appl. Phys. Lett.* **87**, 082501 (2005).
- ¹⁵ K. Petukhov, W. Wernsdorfer, A. L. Barra, and V. Mosser, *Phys. Rev. B* **72**, 052401 (2005).
- ¹⁶ W. Wernsdorfer, D. Mailly, G. A. Timco, and R. E. P. Winpenny, *cond-mat/0504416* (2005).
- ¹⁷ R. Caciuffo, C. Amoretti, A. Murani, R. Sessoli, A. Caneschi, and D. Gatteschi, *Phys. Rev. Lett.* **81**, 4744-4747 (1998).
- ¹⁸ A. L. Barra, D. Gatteschi, and R. Sessoli, *Chem. Eur. J.* **6**, 1608-1614 (2000).
- ¹⁹ A. A. Mukhin, B. Gorshunov, M. Dressel, C. Sangregorio, and D. Gatteschi, *Phys. Rev. B* **63**, 214411 (2001).
- ²⁰ M. Mola, S. Hill, P. Goy, and M. Gross, *Rev. Sci. Instrum.* **71**, 186-200 (2000).
- ²¹ C. P. Poole, Jr., *Electron Spin Resonance, A Comprehensive Treatise on Experimental Techniques*, 2nd ed. (Wiley-Interscience, New York, 1983).
- ²² We note that the energy eigenstates are not pure m states because of the large angle between the external magnetic field and the easy axis of Fe_8 crystal, as well as because of transverse anisotropy terms in the Hamiltonian. However, the magnetic field used in this work (0.19 T) is small relative to the anisotropy fields and therefore does not result in any significant mixing of the eigenstates. For example, we calculate the difference between the mixed eigenstate and the pure $m = 10$ ($m = 9$) state to be 0.37 % (1.25 %) for an angle of 45 $^\circ$.